Research Article | Vol. 25, No. 13 | 26 Jun 2017 | OPTICS EXPRESS 14856
Optics EXPRESS

Scalar and electromagnetic nonparaxial bases composed as superpositions of simple vortex fields with complex foci

RODRIGO GUTIÉRREZ-CUEVAS* AND MIGUEL A. ALONSO

Center for Coherence and Quantum Optics and The Institute of Optics, University of Rochester, Rochester, New York 14627, USA
*rgutier2@ur.rochester.edu

Abstract: We derive bases constructed from simple vortices and complex focus fields and show that they are useful in the description of strongly focused fields. Both scalar and electromagnetic fields are considered, and in each case two types of basis are discussed: bases that use standard polynomials but whose orthogonality condition requires a non-uniform directional weight factor, and bases that are orthogonal with uniform weight but that require new polynomials. Their performance is studied by fitting prescribed fields, where it is seen that the accuracy provided by both types of bases is comparable.

© 2017 Optical Society of America

OCIS codes: (260.1960) Diffraction theory; (070.7345) Wave propagation; (260.2110) Electromagnetic optics; (260.6042) Singular optics; (050.4865) Optical vortices; (260.5430) Polarization.

References and links

1. M. Born and E. Wolf, *Principles of Optics* (Elsevier, 1980).
2. L. Novotny and B. Hecht, *Principles of Nano-Optics* (Cambridge University, 2012).
3. J. Durnin, "Exact solutions for nondiffracting beams. I. The scalar theory," J. Opt. Soc. Am. A **4**, 651–654 (1987).
4. J. . Durnin, J. J. Miceli Jr, and J. H. Eberly, "Diffraction-free beams," Phys. Rev. Lett. **58**, 1499 (1987).
5. C. J. R. Sheppard and P. Török, "Efficient calculation of electromagnetic diffraction in optical systems using a multipole expansion," J. Mod. Opt. **44**, 803–818 (1997).
6. J. D. Jackson, *Classical Electrodynamics* (Wiley, 1998).
7. R. Borghi, M. Santarsiero, and M. A. Alonso, "Highly focused spirally polarized beams," J. Opt. Soc. Am. A .
8. C. W. McCutchen, "Generalized aperture and the three-dimensional diffraction image," J. Opt. Soc. Am. **54**, 240–244 (1964).
9. C. McCutchen, "Generalized aperture and the three-dimensional diffraction image: erratum," J. Opt. Soc. Am. A **19**, 1721 (2002).
10. J. Lin, O. Rodríguez-Herrera, F. Kenny, D. Lara, and J. Dainty, "Fast vectorial calculation of the volumetric focused field distribution by using a three-dimensional fourier transform," Opt. Express **20**, 1060–1069 (2012).
11. M. V. Berry, "Evanescent and real waves in quantum billiards and gaussian beams," J. Phys. A **27**, L391 (1994).
12. C. J. R. Sheppard and S. Saghafi, "Beam modes beyond the paraxial approximation: a scalar treatment," Phys. Rev. A **57**, 2971 (1998).
13. C. J. R. Sheppard and S. Saghafi, "Electromagnetic gaussian beams beyond the paraxial approximation," J. Opt. Soc. Am. A **16**, 1381–1386 (1999).
14. Y. A. Kravtsov, "Complex rays and complex caustics," Radiophys. Quantum Electron. **10**, 719–730 (1967).
15. G. A. Deschamps, "Gaussian beam as a bundle of complex rays," Electro. Lett. **7**, 684–685 (1971).
16. M. A. Alonso, R. Borghi, and M. Santarsiero, "New basis for rotationally symmetric nonparaxial fields in terms of spherical waves with complex foci," Opt. Express **14**, 6894–6905 (2006).
17. N. J. Moore and M. A. Alonso, "Bases for the description of monochromatic, strongly focused, scalar fields," J. Opt. Soc. Am. A **26**, 1754–1761 (2009).
18. N. J. Moore and M. A. Alonso, "Closed-form bases for the description of monochromatic, strongly focused, electromagnetic fields," J. Opt. Soc. Am. A **26**, 2211–2218 (2009).
19. A. M. Yao and M. J. Padgett, "Orbital angular momentum: origins, behavior and applications," Adv. Opt. Photon. **3**, 161–204 (2011).
20. D. L. Andrews and M. Babiker, *The angular momentum of light* (Cambridge University, 2012).
21. R. Gutiérrez-Cuevas and M. A. Alonso, "Polynomials of Gaussians and vortex-Gaussian beams as complete, transversely confined bases," Opt. Lett. **42**, 2205–2208 (2017).
22. A. J. Devaney and E. Wolf, "Multipole expansions and plane wave representations of the electromagnetic field," J. Math. Phys. **15**, 234–244 (1974).
23. G. Szegö, *Orthogonal Polynomials* (American Mathematical Society, 1967).

#287881 https://doi.org/10.1364/OE.25.014856
Journal © 2017 Received 2 Mar 2017; revised 17 May 2017; accepted 23 May 2017; published 20 Jun 2017

Optics EXPRESS

24. M. A. Alonso and N. J. T. Moore, in *Mathematical Optics: Classical, Quantum, and Computational Methods,* V. Lakshminarayanan, ed. (CRC, 2012), Chap. 4, pp. 97–141.
25. K. Y. Bliokh, M. A. Alonso, E. A. Ostrovskaya, and A. Aiello, "Angular momenta and spin-orbit interaction of nonparaxial light in free space," Phys. Rev. A **82**, 063825 (2010).
26. M. V. Berry, "Optical currents," J. Opt. A: Pure Appl. Opt. **11**, 094001 (2009).
27. M. A. Alonso, "The effect of orbital angular momentum and helicity in the uncertainty-type relations between focal spot size and angular spread," J. Opt. **13**, 064016 (2011).
28. T. Grosjean, D. Courjon, "Smallest focal spots," Opt. Commun. **272**, 314–319 (2007).
29. V. V. Kotlyar, S. S. Stafeev, Y. Liu, L. O'Faolain, and A. A. Kovalev, "Analysis of the shape of a subwavelength focal spot for the linearly polarized light," Appl. Opt. **3**, 330–339 (2013).
30. N. J. Moore and M. A. Alonso, "Closed form formula for mie scattering of nonparaxial analogues of gaussian beams," Opt. Express **16**, 5926–5933 (2008).
31. N. J. Moore and M. A. Alonso, "Mie scattering of highly focused, scalar fields: an analytic approach," J. Opt. Soc. Am. A **33**, 1236–1243 (2016).

1. Introduction

The modeling of strongly focused optical fields and nonparaxial light in general typically relies on expansions of the field in terms of bases of closed-form solutions, such as plane waves [1, 2], Bessel beams [3, 4], or multipoles [5–7]. The problem with these basis sets is that they either are continuous (plane waves and Bessel beams), or their elements are omnidirectional (multipoles), so that a large number of elements is needed when modeling focused fields constrained to a range of directions. When using plane-wave expansions, the computational burden of needing a large number of plane waves can be alleviated given the connection between this basis and Fourier transforms, which have a fast computational implementation. For example, McCutchens [8, 9] showed that plane-wave superpositions can be expressed in terms of three-dimensional Fourier transforms, which can be implemented computationally through FFT algorithms [10]. Nevertheless, there are applications in which it might be more convenient to express a field in terms of only an small number of basis elements, and where the main elements display similar properties as the field, such as orbital or spin angular momenta.

There are only a few known rigorous nonparaxial solutions to the monochromatic wave equation besides those mentioned earlier. A particularly interesting one is what is sometimes referred to as a complex-focus (CF) field [11–13] corresponding to a (scalar or vector) generalization of a Gaussian beam with controllable degree of focusing. This analytic solution results from shifting the focus of a spherical wave to a complex point. The real part of this displacement gives the location of the field's focus; the imaginary part, on the other hand, indicates the main direction of propagation and its magnitude corresponds to the field's Rayleigh range (i.e. its directionality). These CF fields do not present the branch-point singularities of the complex source-point fields [14, 15] proposed earlier. A natural generalization of CF fields are vortex CF (VCF) fields, which carry orbital angular momentum (OAM) around their main axis, and are given by the displacement in an imaginary direction of the product of a spherical wave and a simple vortex of given topological charge.

Several previous articles have sought to take advantage of the directionality of CF fields to construct complete, discrete bases for nonparaxial focused fields. Amongst these, a basis restricted to rotationally-symmetric scalar beams was proposed in [16], in which each member of the basis is a combination of coaxial CF fields with different waist widths. Other bases valid for arbitrary fields were given in [17] for scalar fields and [18] for electromagnetic (transverse vector) fields, in terms of non-standard polynomials. The elements of these bases can be regarded as nonparaxial extensions of the well-known paraxial Laguerre-Gaussian beams.

In this manuscript, we propose new complete basis sets that generalize the significantly more restricted basis in [16], so that they can be used for expanding non-rotationally-symmetric fields, whether they are scalar or electromagnetic. Two types of basis are proposed: one is orthonormal in the angular spectrum (or directional) space, with the downside of requiring the construction

Optics EXPRESS

of non-standard polynomials; the second is orthonormal when a non-uniform weight is used, but has the advantage of being expressible in terms of standard (Legendre or more general Jacobi) orthogonal polynomials. The common attractive feature of these new bases is that they are composed as linear combinations of CF and VCF fields, hence allowing a simple description of strongly focused fields carrying both orbital and spin angular momenta [19, 20]. Just like the bases proposed in [17, 18] are natural nonparaxial extensions of Laguerre-Gaussian beams, the new bases proposed here are the nonparaxial counterparts of the polynomials-of-Gaussians bases proposed recently by the authors [21].

2. Scalar fields

2.1. Background

For simplicity, let us begin with the scalar case, where fields satisfy the Helmholtz equation

$$\nabla^2 U(\mathbf{r}) + k^2 U(\mathbf{r}) = 0, \tag{1}$$

in which a monochromatic time dependence $\exp(-\mathrm{i}\omega t)$ is assumed. As mentioned in the introduction, general solutions to this equation can be written as a superposition of plane waves traveling in all directions $\mathbf{u} = (\sin\theta\cos\phi, \sin\theta\sin\phi, \cos\theta)$:

$$U(\mathbf{r}) = \int_{4\pi} A(\mathbf{u}) \exp(\mathrm{i}k\mathbf{u}\cdot\mathbf{r})\, \mathrm{d}\Omega, \tag{2}$$

where the integration is over the unit sphere of plane-wave directions $\theta \in [0, \pi]$, $\phi \in [0, 2\pi)$ (with evanescent components excluded). The amplitude $A(\mathbf{u})$ is referred to as the angular spectrum (AS). In what follows we set $k = 1$ so that all distances are in units of reduced wavelengths.

In spherical coordinates, separable solutions to Eq. (1) are given by the multipolar fields

$$\Lambda_{l,m}(\mathbf{r}) = 4\pi \mathrm{i}^l \mathrm{j}_l(r) Y_{l,m}(\theta_r, \phi_r), \tag{3}$$

where j_l are the spherical Bessel functions and

$$Y_{l,m}(\theta, \phi) = \sigma_m \sqrt{\frac{(2l+1)(l-m)!}{4\pi(l+m)!}} P_l^{(m)}(\cos\theta) \exp(\mathrm{i}m\phi) \tag{4}$$

are the spherical harmonics with $\sigma_m = \mathrm{sgn}\,(m + 1/2)$ and $P_l^{(m)}$ being the generalized Legendre functions. An attractive aspect of the multipolar basis is that it satisfies simple transformation rules from configuration space to direction space [22]; the AS is itself a spherical harmonic:

$$\Lambda_{l,m}(\mathbf{r}) = \int_{4\pi} Y_{l,m}(\theta, \phi) \exp(\mathrm{i}\mathbf{u}\cdot\mathbf{r})\, \mathrm{d}\Omega. \tag{5}$$

It is clear that these fields constitute a complete orthonormal basis over the sphere of directions, so that any free field can be expanded in terms of this basis guaranteeing a decrease in the truncation error with every additional term included in the expansion. As mentioned earlier, their downside is that due to the omnidirectionality of the elements, convergence can be slow when representing more directional fields whose AS is restricted to a region of the sphere of directions.

This issue was partially addressed in [16], where directionality was imposed using the CF idea. A simple CF field propagating in the positive z direction has an AS proportional to $\exp(q\cos\theta)$, where q is a positive parameter [11, 12]. It is easy to see that this exponential factor imposes directionality by emphasizing plane-wave components traveling at small angles θ with respect to the positive z axis. It is also easy to see that the effect of this exponential factor in the position

Optics EXPRESS

space is that of an imaginary displacement $z \to z - \mathrm{i}q$, given the shift-linear phase relation of Fourier transforms. The AS of the basis elements proposed in [16] have the following form:

$$\mathcal{A}_{l,m}(\mathbf{u};q) = b_{l,m}(q)\exp(q\cos\theta)P_l^{(m)}\left[\cos\Theta(\theta;q)\right]\exp(\mathrm{i}m\phi), \tag{6}$$

where

$$b_{l,m}(q) = \sqrt{\frac{q(2l+1)(l-m)!}{2\pi\sinh(2q)(l+m)!}} \quad \text{and} \quad \cos\Theta(\theta;q) = \frac{\exp(2q\cos\theta) - \cosh 2q}{\sinh 2q}. \tag{7}$$

One can see that in the limit of $q \to 0$ Eq. (6) reduces to the spherical harmonics in Eq. (4) while $q \to \infty$ corresponds to paraxial beams, thus the parameter q controls the degree of directionality of the basis elements. For any q this basis indeed constitutes a complete orthonormal basis over the directional space. However, for it to be useful, its elements must have a relatively simple closed-form expression in configuration space, that is, when their AS is substituted into Eq. (2). This happens to be the case only for rotationally symmetric beams ($m = 0$), because of the problematic factor of $\sin^{|m|}\Theta(\theta;q)$ inherent in the generalized Lengendre functions. This is precisely the reason why this basis is only useful for rotationally symmetric fields.

2.2. Nonorthogonal solution

A simple solution to the problem just outlined is to multiply the AS of the previous basis by an appropriate factor. This factor causes the orthogonality relation in the space of directions to involve a non-uniform weight, but allows the basis elements to be expressible in closed form in terms of standard polynomials. We define the elements of the basis in the directional space as

$$\mathcal{M}_{n,m}(\mathbf{u};q) = b_{n+|m|,m}(q)\exp(q\cos\theta)\left\{\frac{P_{n+|m|}^{(m)}\left[\cos\Theta(\theta;q)\right]}{\sin^{|m|}\Theta(\theta;q)}\right\}\sin^{|m|}\theta\exp(\mathrm{i}m\phi). \tag{8}$$

Note that we replaced the index l with $n + |m|$ so that m can take any integer value, irrespective of n. This choice of indices is used for all subsequent bases derived in this manuscript. The factor in curly brackets is proportional to the Jacobi polynomial $P_n^{(m,m)}\left[\cos\Theta(\theta;q)\right]$ which can be expanded as a sum of terms proportional to $\exp(2jq\cos\theta)$ for $j = 0, 1, \ldots, n$. This shows that the problematic factor has been removed: the expression is now a simple vortex of charge m given by $\sin^{|m|}\theta\exp(\mathrm{i}m\phi)$, times a sum of terms that include CF displacement factors $\exp[(2j+1)q\cos\theta]$. By using the fact that the simple vortex is an extreme ($l = |m|$) spherical harmonic, $\sin^{|m|}\theta\exp(\mathrm{i}m\phi) = c_m Y_{|m|,m}(\theta,\phi)$ with $c_m = (-\sigma_m)^{|m|}2^{|m|}|m|![4\pi/(2|m|+1)!]^{1/2}$, as well as the property of complex displacements applied to simple vortices gives VCF fields,

$$V^{(m)}(\mathbf{r};q) = \Lambda_{|m|,m}[\mathbf{r} - \mathrm{i}q\hat{\mathbf{z}}] = \int Y_{|m|,m}(\theta,\phi)\exp(q\cos\theta)\exp(\mathrm{i}\mathbf{r}\cdot\mathbf{u})\,\mathrm{d}\Omega \tag{9}$$

$$= \frac{4\pi\mathrm{i}^{|m|}}{c_m}\mathrm{j}_{|m|}\left[\sqrt{\rho^2 + (z - \mathrm{i}q)^2}\right]\left[\frac{\rho}{\sqrt{\rho^2 + (z - \mathrm{i}q)^2}}\right]^{|m|}\exp(\mathrm{i}m\phi), \tag{10}$$

with $\rho^2 = x^2 + y^2$, we can find the expression for the basis elements in configuration space as

$$\mathcal{U}_{n,m}(\mathbf{r};q) = \sum_{j=0}^{n} v_{n,m}^{(j)} V^{(m)}[\mathbf{r};(2j+1)q], \tag{11}$$

where $v_{n,m}^{(j)} = b_{n+|m|,m}(q)c_m p_{n,m}^{(j)}$ with $p_{n,m}^{(j)}$ being the coefficient of the j^{th} power of the polynomial $P_{n+|m|}^{(m)}[(x - \cosh 2q)/\sin 2q]/\sin^{|m|}[(x - \cosh 2q)/\sin 2q]$. That is, each basis

Optics EXPRESS

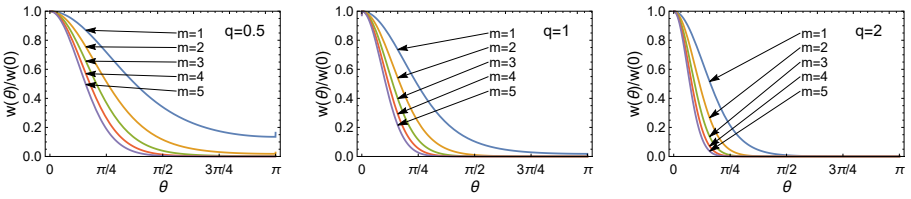

Fig. 1. Normalized weight function for the nonorthogonal nonparaxial scalar basis, Eq. (12), for different values of m and q.

element is just a linear combination of VCF fields $V^{(m)}$ with definite vorticity m and different imaginary displacements $(2j+1)q$ in the positive z direction.

As mentioned earlier, for the elements of this basis to be orthonormal in the directional space, the following m-dependent weight factor must be used over the directional polar angle:

$$W_m(\theta) = \left[\sin\Theta(\theta;q)/\sin\theta\right]^{|2m|}. \tag{12}$$

Figure 1 shows this weight for different values of m and q. Its behavior is analogous to the one for the paraxial modified Gauss-Legendre basis [21]: as $|m|$ increases, the weight becomes localized around the positive z direction. A similar behavior takes place with q for all values of $m \neq 0$. Because the basis should be used to fit sufficiently directional fields propagating in the positive z direction, this directional localization factor should not affect significantly the basis' convergence under truncation of the sum. It is also worth noting that, in the limit $q \to 0$, $W_m \to 1$ and this basis reduces to the multipoles in Eq. (3). Visualization 1 shows the transition from the multipoles ($q = 0$) to highly directional beams ($q = 10$) for four elements of the basis.

2.3. Orthogonal solution

Noting the simple relation between the directional and configuration spaces satisfied by the previous basis, we can define an alternative basis with essentially the same form but with the added feature of being orthogonal without requiring a weight factor. The downside is that it requires the construction of new polynomials by the method of moments [23,24] (see Appendix A). In the directional space, the elements of this basis have a similar form to that in Eq. (8):

$$\mathcal{G}_{n,m}(\mathbf{u};q) = g_{n,m}(q)\exp(q\cos\theta)G_{n,m}[\exp(2q\cos\theta);q]\sin^{|m|}\theta\exp(\mathrm{i}m\phi), \tag{13}$$

where the functions $G_{n,m}$ are orthogonal polynomials that are now defined. The change of variable $v = \exp(2q\cos\theta)$ leads to the following orthogonality condition for these polynomials:

$$\int_{\exp(-2q)}^{\exp(2q)} G_{n',m}(v;q)G_{n,m}(v;q)w_m(v)\,\mathrm{d}v = h_{n,m}(q)\delta_{n,n'},\ w_m(v) = \left(1-\frac{\ln^2 v}{4q^2}\right)^{|m|}. \tag{14}$$

The normalization coefficient can be written as $g_{n,m}(q) = [q/\pi h_{n,m}(q)]^{1/2}$, where $h_{n,m}(q)$ (explained in Appendix A) is the norm of the polynomials. Figures 2(a) and 2(b) show the θ dependence of the AS for different orders. We note that all orders have roughly the same angular extent (similarly to the paraxial bases in [21]), which is regulated by q: the larger q, the more concentrated the AS is around the forward direction $\theta = 0$.

As in Section 2.2, the polynomials give a series of terms with exponentials $\exp[(2j+1)q\cos\theta]$, so the basis elements in configuration space can be expressed as sums of VCF fields:

$$\mathcal{U}_{n,m}(\mathbf{r};q) = g_{n,m}(q)\sum_{j=0}^{n}\gamma_{n,m}^{(j)}(q)c_m V^{(m)}[\mathbf{r};(2j+1)q], \tag{15}$$

Optics EXPRESS

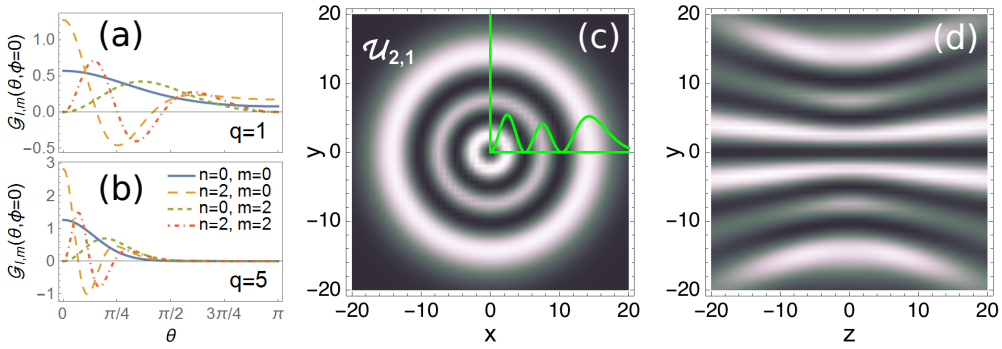

Fig. 2. (a,b) θ dependence of $\mathcal{G}_{n,m}$ for $\phi = 0$ for different orders and values of q. (c,d) Intensity over the x-y plane (c) and the y-z plane (d) for the orthogonal basis element $\mathcal{U}_{2,1}$ with $q = 10$. The green curve on the x-y plane shows the intensity profile along the x axis.

where $\gamma^{(j)}_{n,m}(q)$ is the coefficient corresponding to the j^{th} power in the polynomial $G_{n,m}$. Two intensity profiles are shown in Figs. 2(c) and 2(d) for the basis element with $n = 2$, $m = 1$, and $q = 10$.

Note that, like Eq. (8), the AS basis in Eq. (13) reduces to the spherical harmonics when $q \to 0$. [For the orthogonal basis, this can be seen by expressing the polynomials $G_{n,m}$ in terms of $\cos\Theta(\theta; q)$, which changes the limits of integration in Eq. (14) to ± 1, and then taking the limit.] Therefore, both of the new bases coincide with the monopoles in Eq. (3) when $q = 0$. Note also that, for any q, the elements of the two new bases coincide for $m = 0$.

2.4. *Comparing the bases: fitting prescribed fields*

We now apply and compare the two new bases for a specific example. Since they are identical for $m = 0$, we consider an example that is not rotationally symmetric. A field with AS given by $A(\mathbf{u})$ can be approximated in terms of a basis, say $\mathcal{Y}_{n,m}$, as the truncated expansion

$$\widetilde{A}(\mathbf{u}) = \sum_{n=0}^{n_{\max}} \sum_{m=-m_{\max}}^{m_{\max}} a_{n,m} \mathcal{Y}_{n,m}(\mathbf{u}) \tag{16}$$

where $\widetilde{A}$ is the approximated field with truncation orders $n_{\max}$ and $m_{\max}$. The coefficients are found through

$$a_{n,m} = \int_{4\pi} A(\mathbf{u}) \mathcal{Y}^*_{n,m}(\mathbf{u}) W_m(\theta)\, \mathrm{d}\Omega \tag{17}$$

with $W_m(\theta)$ being the appropriate directional weight. The resulting rms truncation error is

$$\epsilon^2_{\text{rms}} = \frac{\int_{4\pi} |A(\mathbf{u}) - \widetilde{A}(\mathbf{u})|^2\, \mathrm{d}\Omega}{\int_{4\pi} |A(\mathbf{u})|^2\, \mathrm{d}\Omega}. \tag{18}$$

This expression takes a simple form for orthonormal bases

$$\epsilon^2_{\text{rms}} = 1 - \frac{\sum_{n=0}^{n_{\max}} \sum_{m=-m_{\max}}^{m_{\max}} |a_{n,m}|^2}{\int_{4\pi} |A(\mathbf{u})|^2\, \mathrm{d}\Omega}. \tag{19}$$

We consider an elliptical Gaussian beam which has a ϕ dependent waist focused by a thin lens. For this field the plane-wave amplitude is given by

$$A(\mathbf{u}) = \exp\left[-\frac{\tan^2\theta}{2\Delta^2(1 + \delta w \cos 2\phi)^2}\right] \frac{H(\theta - \pi/2)}{\cos\theta}, \tag{20}$$

Optics EXPRESS

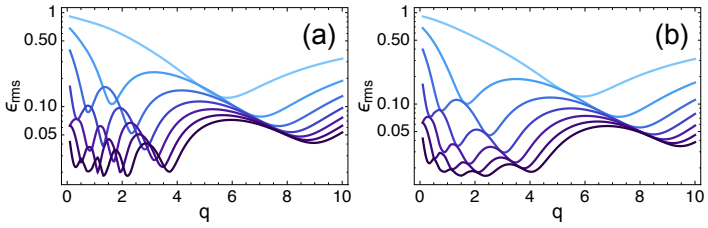

Fig. 3. Rms error as a function of q for an elliptical Gaussian beam focused by a thin lens with $\Delta = 0.5$ and $\delta w = 0.2$ (a) for the modified basis $\mathcal{M}_{n,m}$, and (b) the orthogonal basis $\mathcal{G}_{n,m}$ for truncation orders $n_{\max} = 0$ (lighter curves) to $n_{\max} = 6$ (darker curves).

where H is the Heaviside function. Due to the symmetry of the field, all coefficients for odd m vanish. The rms error is computed for different orders while varying the free parameter q. Figure 3 shows the resulting error curves as a function of q for the two bases derived in the previous section for $\Delta = 0.5$ and $\delta w = 0.2$. The maximum value of $|m|$ was fixed to 2 and each curve was obtained with a fit which used $3(n_{\max} + 1)$ elements of the basis, adding contributions each time with $m = 0, \pm 2$. Note that, even though the nonorthogonality is made evident in Fig. 3(a) by the crossings in the error curve, the minimum error attained is comparable to that of the orthogonal basis. This same case was studied in [17] using a different basis and by comparing the results we see that the present bases perform better. Additionally the optimum q stays somewhat fixed with increasing order while for the bases in [17] it shifts toward higher values. This behavior is analogous to that of the paraxial bases presented in [21] when compared to the standard Laguerre-Gauss basis.

This example shows the usefulness of the two bases presented here when fitting focused beams. The complex displacement introduces directionality into the basis elements that allows reducing significantly the errors with respect to those for the standard multipolar basis, which correspond to the values for $q = 0$ in both plots. Note that the error presents an oscillatory behavior in terms of q, where each curve has a number of local minima equal to $n_{\max} + 1$. These oscillations are typical of variations of a scaling parameter, and also occur, for example, when using a Hermite-Gaussian basis to fit a real function. The local minima correspond approximately to the values of the scaling for which the leading basis element that is being dropped happens to be orthogonal to the fitted function. (Similarly, the local maxima correspond roughly to the values of q for which the highest order term being used is orthogonal to the fitted function.) These oscillations would not be so pronounced (or would even disappear) if the fitted angular spectrum had, for example, a θ dependent phase, since the leading dropped basis element could not be orthogonal to both the real and imaginary parts simultaneously. This happens, for example, when fitting a field with spherical aberration.

3. Electromagnetic fields

3.1. Background

We now proceed to the electromagnetic case where fields are solutions of the vector Helmholtz equation with an added transversality condition:

$$\nabla^2 \mathbf{E}(\mathbf{r}) + \mathbf{E}(\mathbf{r}) = 0, \qquad \nabla \cdot \mathbf{E}(\mathbf{r}) = 0. \tag{21}$$

As before, a general solution for a source-free field can be decomposed in terms of plane waves,

$$\mathbf{E}(\mathbf{r}) = \int_{4\pi} \mathbf{A}(\mathbf{u}) \exp(\mathrm{i}\mathbf{u} \cdot \mathbf{r}) \, \mathrm{d}\Omega, \tag{22}$$

Optics EXPRESS

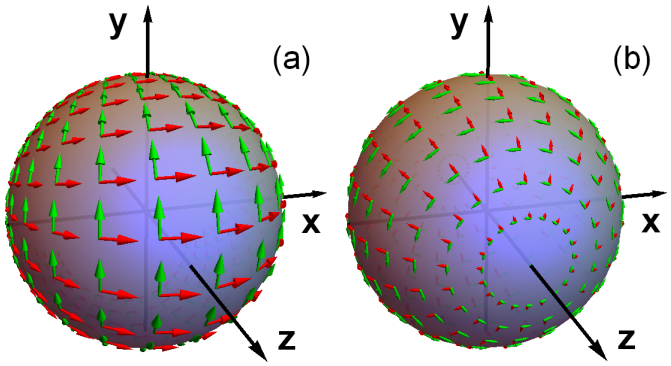

Fig. 4. Polarization vectors $\mathbf{V_u}$ and $\mathbf{u} \times \mathbf{V_u}$ for the (a) quasi-linear and (b) TE-TM bases.

where $\mathbf{A}(\mathbf{u})$ is the vectorial AS, for which the divergence condition takes the form: $\mathbf{u} \cdot \mathbf{A}(\mathbf{u}) = 0$.

Vector solutions in spherical coordinates can be expressed in terms of the vector multipoles $\mathbf{\Lambda}^{(\mathrm{I})}_{l,m}$ and $\mathbf{\Lambda}^{(\mathrm{II})}_{l,m}$, which form a complete basis for free monochromatic electromagnetic fields. In the directional space, these can be written as [22]

$$\mathbf{\Lambda}^{(\mathrm{I})}_{l,m}(\mathbf{r}) = \int_{4\pi} \mathbf{Z}_{l,m}(\mathbf{u}) \exp(\mathrm{i}\mathbf{u}\cdot\mathbf{r})\, \mathrm{d}\Omega, \quad \mathbf{\Lambda}^{(\mathrm{II})}_{l,m}(\mathbf{r}) = \int_{4\pi} \mathbf{Y}_{l,m}(\mathbf{u}) \exp(\mathrm{i}\mathbf{u}\cdot\mathbf{r})\, \mathrm{d}\Omega, \tag{23}$$

where we used the vector spherical harmonics, which are defined as

$$\mathbf{Z}_{l,m}(\mathbf{u}) = \mathbf{u} \times \mathbf{Y}_{l,m}(\mathbf{u}), \qquad \mathbf{Y}_{l,m}(\mathbf{u}) = \frac{1}{\sqrt{l(l+1)}} \mathbf{L_u} Y_{l,m}(\theta, \phi), \tag{24}$$

given the angular momentum operator

$$\mathbf{L_u} = -\mathrm{i}\mathbf{u} \times \nabla_\Omega = -\mathrm{i}\mathbf{u} \times \left(\frac{\hat{\boldsymbol{\phi}}}{\sin\theta} \frac{\partial}{\partial\phi} + \hat{\boldsymbol{\theta}} \frac{\partial}{\partial\theta} \right) = \mathrm{i} \frac{\hat{\boldsymbol{\theta}}}{\sin\theta} \frac{\partial}{\partial\phi} - \mathrm{i}\hat{\boldsymbol{\phi}} \frac{\partial}{\partial\theta}, \tag{25}$$

with $\hat{\boldsymbol{\theta}}$ and $\hat{\boldsymbol{\phi}}$ being the unit vectors in the polar and azimuthal directions, respectively. As in the scalar case, this basis is suitable for describing fields with components in most of the 4π steradian solid angles thus leading to a slow convergence for more directional fields. In this case, the orthonormal basis is presented first, followed by its nonorthogonal counterpart which uses standard polynomials.

3.2. Orthogonal basis

The electromagnetic analogue of the basis derived in Section 2.3 follows from assuming the same type of functional form:

$$\mathcal{G}_{n,m}(\mathbf{u}; q) = \mathbf{V_u} \mathscr{G}_{n,m}(\mathbf{u}; q), \qquad \mathcal{Z}_{n,m}(\mathbf{u}; q) = \mathbf{u} \times \mathbf{V}^\dagger_{\mathbf{u}} \mathscr{G}_{n,m}(\mathbf{u}; q), \tag{26}$$

with

$$\mathscr{G}_{n,m}(\mathbf{u}; q) = g_{n,m}(q) \exp(q\cos\theta) G_{n,m}[\exp(2q\cos\theta); q] \sin^{|m|}\theta \exp(\mathrm{i}m\phi), \tag{27}$$

where the $G_{n,m}$ are some polynomials that need to be identified or constructed. The vector $\mathbf{V_u}$ (which is in general an operator) needs to satisfy $\mathbf{u} \cdot \mathbf{V_u} = 0$ and $\mathbf{u} \times \mathbf{V}^\dagger_{\mathbf{u}} = -\mathbf{V}^\dagger_{\mathbf{u}} \times \mathbf{u}$ to guarantee the transversality of the fields as well as

$$\int_{4\pi} \mathcal{G}^*_{n',m'}(\mathbf{u}; q) \cdot \mathcal{Z}_{n,m}(\mathbf{u}; q)\, \mathrm{d}\Omega = 0, \tag{28}$$

Optics EXPRESS

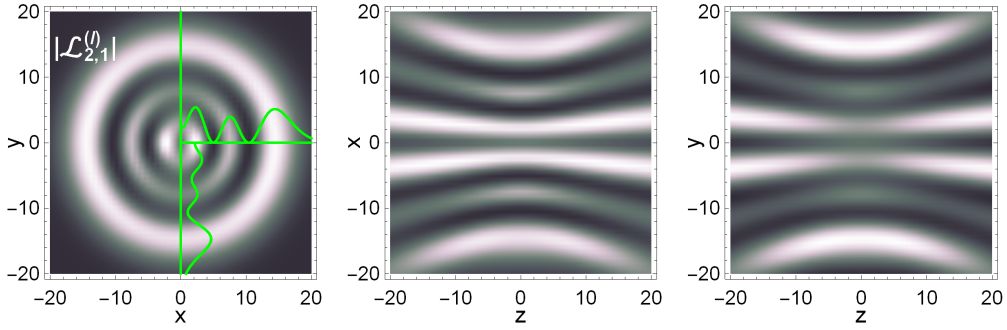

Fig. 5. Intensity over (left) the x-y plane, (center) x-z, and (right) the y-z plane for the orthogonal basis element $\mathcal{L}^{(\mathrm{I})}_{2,1}$ with $q = 10$. The green curves on the x-y plane show the intensity profile along the x and y axes.

and

$$\int_{4\pi} \mathcal{G}^{*}_{n',m'}(\mathbf{u};q)\cdot\mathcal{G}_{n,m}(\mathbf{u};q)\,\mathrm{d}\Omega = \int_{4\pi} \mathcal{Z}^{*}_{n',m'}(\mathbf{u};q)\cdot\mathcal{Z}_{n,m}(\mathbf{u};q)\,\mathrm{d}\Omega. \tag{29}$$

Since there is no obvious choice for the $G_{n,m}$ polynomials, we proceed by demanding orthogonality within each set of the basis elements. Making the change of variables $v = \exp(2q\cos\theta)$ leads to the following orthogonality condition for the polynomials:

$$\int_{\exp(-2kq)}^{\exp(2kq)} G_{n',m}(v;q)\hat{w}_m(v;q)G_{n,m}(v;q)\,\mathrm{d}v = h_{n,m}(q)\delta_{n',n} \tag{30}$$

where the weight is, in general, an operator that must be independent of ϕ and will depend on our choice of the vector $\mathbf{V_u}$. The normalization coefficient can again be written as $g_{n,m}(q) = [q/\pi h_{n,m}(q)]^{1/2}$.

There are several options for the vector $\mathbf{V_u}$ such as the ones presented in [18]; here we focus on the one referred to as quasi-linear, since it does not have polarization singularities except at the negative z direction [see Fig. 4(a)] and thus allows a simple description of most standard states of polarization. Hence, $\mathbf{V_u} = \mathbf{u}\times\hat{\mathbf{x}}\times\mathbf{u} - \mathbf{u}\times\hat{\mathbf{y}}$ for which $\mathbf{V}^{\dagger}_{\mathbf{u}}\mathbf{V_u} = (1+\cos\theta)^2$, and the weight takes the non-operational (so we drop the hat in w) form

$$w_m(v;q) = \left(1+\frac{1}{2q}\ln v\right)^2\left(1-\frac{1}{4q^2}\ln^2 v\right)^{|m|}. \tag{31}$$

The polynomials are then constructed using the method in Appendix A.

As in the scalar case, for the basis to be useful its elements must have relatively simple-closed-form expressions in configuration space. Following similar steps, we find

$$\mathcal{L}^{(\mathrm{II})}_{n,m}(\boldsymbol{r};q) = \int_{4\pi}\mathcal{G}_{n,m}(\mathbf{u};q)\exp(\mathrm{i}\mathbf{u}\cdot\mathbf{r})\,\mathrm{d}\Omega = \sum_{j=0}^{n}\alpha^{(j)}_{n,m}(q)\mathbf{V_r}V^{(m)}[\mathbf{r};(2j+1)q], \tag{32}$$

and analogously for $\mathcal{L}^{(\mathrm{I})}_{n,m}(\boldsymbol{r};q)$ with $-\mathrm{i}\nabla\times\mathbf{V_r}$ instead of $\mathbf{V_r}$. Here, $\alpha^{(j)}_{n,m}(q) = g_{n,m}(q)\gamma^{(j)}_{n,m}(q)c_m$ with $\gamma^{(j)}_{n,m}(q)$ being the coefficient corresponding to the j^{th} power of the polynomial $G_{n,m}$. The position representation of the polarization operators $\mathbf{V_u}$ and $\mathbf{u}\times\mathbf{V_u}$ is easily derived by substituting $\mathbf{u}\to\nabla/\mathrm{i}$, namely

$$\mathbf{V_u}\to\mathbf{V_r} = \hat{\mathbf{x}} + \nabla\partial_x - \mathrm{i}\hat{\mathbf{y}}\times\nabla, \qquad \mathbf{u}\times\mathbf{V_u}\to -\mathrm{i}\nabla\times\mathbf{V_r} = \hat{\mathbf{y}} + \nabla\partial_y + \mathrm{i}\hat{\mathbf{x}}\times\nabla. \tag{33}$$

Optics EXPRESS

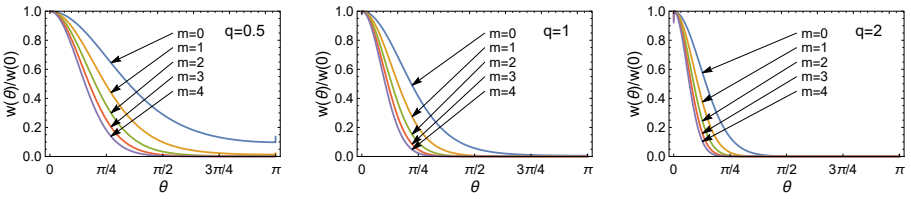

Fig. 6. Normalized weight function for the nonorthogonal electromagnetic basis, Eq. (41), for different values of m and q.

Therefore, the electromagnetic basis is obtained from a scalar basis (with slightly different polynomials) by simply applying the polarization operators. Thus, in configuration space, the elements of the basis inherit the simplicity of the scalar case and only involve derivatives of VCFs with different imaginary displacements. As an example, Fig. 5 shows the intensity profile for the basis element $\boldsymbol{\mathcal{L}}^{(1)}_{2,1}$, we readily notice that the intensity is no longer strictly rotationally symmetric due to the effects of polarization.

3.3. Nonorthogonal basis

We can also find electromagnetic bases in terms of standard polynomials. Let us write the polynomial in Eq. (27) in terms of $\cos\Theta(\theta;q)$ [as defined in Eq. (7)] so that

$$\mathscr{Q}_{n,m}(\mathbf{u};q) = p_{n,m}(q)\exp(q\cos\theta)Q_{n,m}[\cos\Theta(\theta;q)]\sin^{|m|}\theta\exp(\mathrm{i}m\phi) \tag{34}$$

instead of $\mathscr{G}_{n,m}$ in Eqs. (26). It is now easy to realize that in the limit $q\to 0$ this becomes

$$\mathscr{Q}_{n,m}(\mathbf{u};0) = p_{n,m}(0)Q_{n,m}(\cos\theta)\sin^{|m|}\theta\exp(\mathrm{i}m\phi). \tag{35}$$

Therefore, if this basis were to be orthogonal (in this limit) then it would need to satisfy

$$\int_{4\pi}\mathscr{Q}^{*}_{n',m'}(\mathbf{u};0)\mathbf{V}^{\dagger}_{\mathbf{u}}\mathbf{V}_{\mathbf{u}}\mathscr{Q}_{n,m}(\mathbf{u};0)\,\mathrm{d}\Omega = \delta_{n,n'}\delta_{m,m'}. \tag{36}$$

Making the change of variable $s=\cos\theta$, this becomes

$$\int_{-1}^{1}Q_{n',m}(s)Q_{n,m}(s)\,(1-s)^{|m|}\,(1+s)^{|m|+2}\,\mathrm{d}s = \frac{\delta_{n,n'}}{2\pi|p_{n,m}(0)|^2}, \tag{37}$$

which we recognize as the orthogonality condition for the Jacobi polynomials $P_n^{(|m|,|m|+2)}$. Thus, we present the basis

$$\boldsymbol{\mathcal{Q}}_{n,m}(\mathbf{u};q) = \mathbf{V}_{\mathbf{u}}\mathscr{Q}_{n,m}(\mathbf{u};q), \qquad \boldsymbol{\mathcal{X}}_{n,m}(\mathbf{u};q) = \mathbf{u}\times\mathbf{V}^{\dagger}_{\mathbf{u}}\mathscr{Q}_{n,m}(\mathbf{u};q), \tag{38}$$

with

$$\mathscr{Q}_{n,m}(\mathbf{u};q) = p_{n,m}(q)\exp(q\cos\theta)P_n^{(|m|,|m|+2)}[\cos\Theta(\theta;q)]\sin^{|m|}\theta\exp(\mathrm{i}m\phi), \tag{39}$$

where

$$p_{n,m}(q) = \sqrt{\frac{qn!(2n+2|m|+3)(n+2|m|+2)!}{2^{2|m|+3}\pi\sinh(2q)(n+|m|)!(n+|m|+2)!}}. \tag{40}$$

Since we chose the same type of structure as in the orthogonal case, this basis has an analogous simple expression in configuration space. Like the scalar basis in Section 2.2, this is not orthogonal when all directions are weighted equally, even when $m=0$, as long as $q\neq 0$. However, as we

Optics EXPRESS

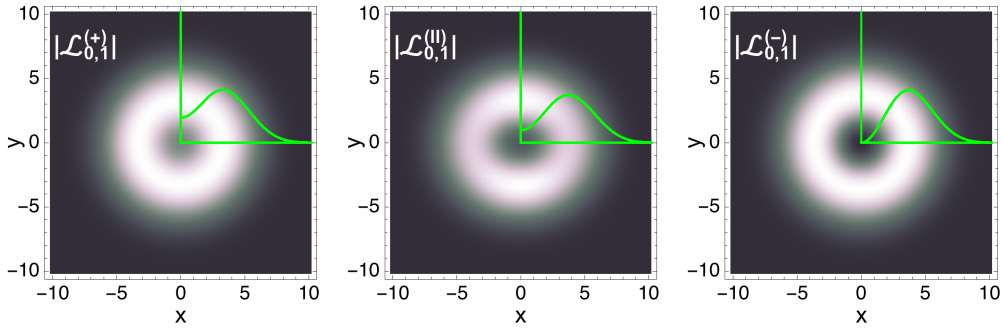

Fig. 7. Magnitude over the x-y plane and the x axis (green curve) for the polarized fields $\mathcal{L}^{(+)}_{n,m}$, $\mathcal{L}^{(II)}_{n,m}$ and $\mathcal{L}^{(+)}_{n,m}$ with $n = 0$, $m = 1$ and $q = 10$.

have already mentioned, in this case orthogonality is just for mathematical convenience. As we showed for the scalar case, there does not seem to be a big difference in performance between the orthogonal and nonorthogonal cases, so we expect the same to be true for the vectorial basis. One can show that this basis is orthogonal with respect to the weight function

$$W_m(\theta) = \frac{[1-\cos\Theta(\theta;q)]^{|m|}[1+\cos\Theta(\theta;q)]^{|m|+2}}{(1-\cos\theta)^{|m|}(1+\cos\theta)^{|m|+2}} \tag{41}$$

which is plotted in Fig. 6 for different values of m and q. Again, as $|m|$ or q increase the weight function concentrates around the forward propagation.

3.4. Helicity basis

From the quasi-linear basis used in the previous section, we can build the analogous quasi-circular basis in which the elements have definite helicity. This is done by taking

$$\mathbf{V}^{(\pm)}_{\mathbf{u}} = \frac{\exp(\mathrm{i}\pi/4)}{\sqrt{2}}(\mathbf{V}_{\mathbf{u}} \pm \mathrm{i}\mathbf{u}\times\mathbf{V}_{\mathbf{u}}) = \exp(\mathrm{i}\pi/4)(\mathbf{u}\times\boldsymbol{\epsilon}_{\pm}\times\mathbf{u} \pm \mathrm{i}\mathbf{u}\times\boldsymbol{\epsilon}_{\pm}), \tag{42}$$

where $\boldsymbol{\epsilon}_{\pm} = 2^{-1/2}(\hat{\mathbf{x}} \pm \mathrm{i}\hat{\mathbf{y}})$ are the paraxial helicity vectors and $\mathbf{V}^{(-)}_{\mathbf{u}} = \mathbf{u}\times\mathbf{V}^{(+)\dagger}_{\mathbf{u}}$. Note that if we write the polarization vectors in terms of the polar and azimuthal unit vectors we have that

$$\mathbf{V}^{(\pm)}_{\mathbf{u}} = \frac{1+\cos\theta}{\sqrt{2}}\exp(\mathrm{i}\pi/4)\exp(\pm\mathrm{i}\phi)(\hat{\boldsymbol{\theta}} \pm \mathrm{i}\hat{\boldsymbol{\phi}}), \tag{43}$$

correspond to the helicity vectors in [25] with $m = 1$, which prevents a phase singularity in the positive z direction, so the basis is well suited for modeling the total angular momentum carried by nonparaxial fields as well as for computations of torques imparted to spherical particles.

These polarization vectors also satisfy $\mathbf{V}^{(\pm)\dagger}_{\mathbf{u}}\mathbf{V}^{(\pm)}_{\mathbf{u}} = (1+\cos\theta)^2$, hence the same polynomials as in the quasi-linear bases can be used, and the elements of this basis in directional space are obtained by applying the polarization operators $\mathbf{V}^{(\pm)}_{\mathbf{u}}$ to Eqs. (27) or (39) depending which basis we want (orthogonal or nonorthogonal). The elements in configuration space are obtained by transforming the polarization vector:

$$\mathbf{V}^{(\pm)}_{\mathbf{r}} = \exp(\mathrm{i}\pi/4)\left[\boldsymbol{\epsilon}_{\pm} + \nabla(\boldsymbol{\epsilon}_{\pm}\cdot\nabla) \mp \boldsymbol{\epsilon}_{\pm}\times\nabla\right]. \tag{44}$$

Using a helicity basis allows us, for example, to visualize the phenomenon of spin-orbit coupling for nonparaxial fields. In the paraxial case it is easy to separate the total angular

Optics EXPRESS

momentum into the contributions from the spin (i. e. polarization) and orbital parts, but as soon as we enter the nonparaxial regime this separation is not straightforward [25–27]. This spin-orbit interaction is exemplified in Fig. 7, which shows the magnitude of the fields $\boldsymbol{\mathcal{L}}^{(+)}_{n,m}$ and $\boldsymbol{\mathcal{L}}^{(-)}_{n,m}$ obtained form the polarization operators $\mathbf{V}^{(\pm)}_{\mathbf{r}}$ along with the linear field $\boldsymbol{\mathcal{L}}^{(\mathrm{II})}_{n,m}$ for $n = 0$ and $m = 1$ across the x-y plane. We notice a clear difference in the radial profile of the field for each circular polarization.

Note that for focused fields the polarization plays an important role in determining the intensity profile, even when there is no spin-orbit coupling. This is clearly seen in Fig. 5 and the central panel of Fig. 7 where the linear polarization breaks the rotational symmetry (present in the paraxial regime) in the intensity distribution. As a consequence, the shape and size of the focal spot is affected [28, 29]. Hence, these bases would be useful to study how the focal point of a given field is shaped by polarization and orbital angular momentum and, particularly, how it is affected when changing the degree of directionality of the field (the transition between paraxial and nonparaxial).

3.5. Comparing the bases: fitting prescribed fields

Let us test the performance of these bases when approximating a prescribed field. The approximated field can be calculated as

$$\widetilde{\mathbf{A}}(\mathbf{u}) = \sum_{n=0}^{n_{\max}} \sum_{m=-m_{\max}}^{m_{\max}} [c^{(\mathrm{I})}_{n,m} \boldsymbol{\mathcal{Z}}_{n,m}(\mathbf{u}) + c^{(\mathrm{II})}_{n,m} \boldsymbol{\mathcal{G}}_{n,m}(\mathbf{u})] \tag{45}$$

where the coefficients are computed by means of the following equations:

$$c^{(\mathrm{I})}_{n,m} = \int_{4\pi} \boldsymbol{\mathcal{Z}}^{*}_{n,m}(\mathbf{u}) \cdot \mathbf{A}(\mathbf{u}) W_m(\theta)\, \mathrm{d}\Omega, \quad c^{(\mathrm{II})}_{n,m} = \int_{4\pi} \boldsymbol{\mathcal{G}}^{*}_{n,m}(\mathbf{u}) \cdot \mathbf{A}(\mathbf{u}) W_m(\theta)\, \mathrm{d}\Omega. \tag{46}$$

To measure the accuracy of the approximation we use the rms truncation error defined as

$$\epsilon_{\mathrm{rms}} = \frac{\|\mathbf{A} - \widetilde{\mathbf{A}}\|}{\|\mathbf{A}\|}, \qquad \|\mathbf{A}\|^2 = \int_{4\pi} \mathbf{A}^{*}(\mathbf{u}) \cdot \mathbf{A}(\mathbf{u})\, \mathrm{d}\Omega. \tag{47}$$

As before, this expression is simplified for the case of an orthonormal basis with uniform directional weight,

$$\epsilon^2_{\mathrm{rms}} = 1 - \frac{\sum_{n=0}^{n_{\max}} \sum_{m=-m_{\max}}^{m_{\max}} [|c^{(\mathrm{I})}_{n,m}|^2 + |c^{(\mathrm{II})}_{n,m}|^2]}{\|\mathbf{A}\|^2}. \tag{48}$$

We borrow an example from [18], namely a collimated paraxial beam being focused down at its waist plane by a thin lens, with focal length f, free of spherical aberration. We take into account the different transmission coefficients for radial and azimuthal components. Therefore, for $\theta \geq \pi/2$ we have

$$\mathbf{A}(\mathbf{u}) = \frac{1}{\cos\theta} [\hat{\boldsymbol{\theta}} T_{\parallel}(\theta) E^{(i)}_{\rho}(f \tan\theta, \phi, 0) + \hat{\boldsymbol{\phi}} T_{\perp}(\theta) E^{(i)}_{\phi}(f \tan\theta, \phi, 0)] \tag{49}$$

where $E^{(i)}_{\rho}$ and $E^{(i)}_{\phi}$ are the radial and azimuthal components of the incident beam, respectively, and the Fresnel coefficients are

$$T_{\parallel}(\theta) = \frac{4 \sin\theta}{\sin(3\theta/2)\cos(\theta/2)}, \qquad T_{\perp}(\theta) = \frac{4 \sin\theta \cos(\theta/2)}{\sin(3\theta/2)}. \tag{50}$$

Optics EXPRESS

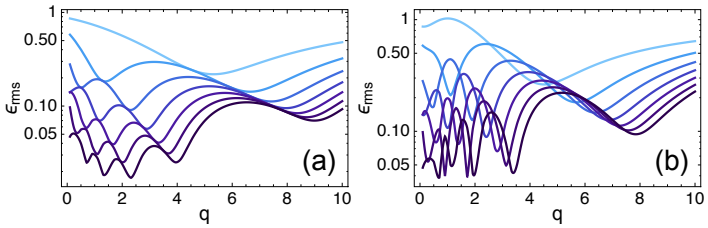

Fig. 8. Rms error as a function of q for a focused radially-polarized Laguerre-Gauss beam of order one with $\Delta = 0.5$ (a) for the orthogonal, and (b) the nonorthogonal bases with truncation orders ranging from $n_{\max} = 0$ (lighter curves) to $n_{\max} = 6$ (darker curves) and $m = -1, 1$.

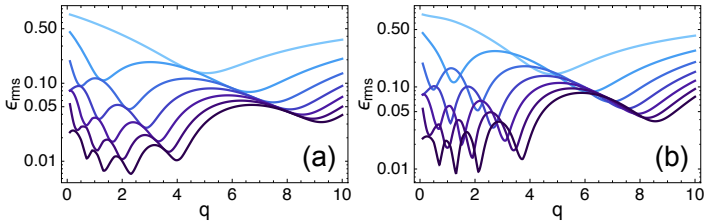

Fig. 9. Rms error as a function of q for a focused linearly-polarized Gaussian beam of order one with $\Delta = 0.5$ (a) for the orthogonal, and (b) the nonorthogonal bases with truncation orders ranging from $n_{\max} = 0$ (lighter curves) to $n_{\max} = 6$ (darker curves) and $m = -2, 0, 2$.

For $\theta > \pi/2$, $\mathbf{A}(\mathbf{u}) = 0$. We consider two incident beams: a radially polarized Laguerre-Gauss beam of order one,

$$\mathbf{E}^{(i)}(\rho, \phi, 0) = E_0 \hat{\boldsymbol{\rho}} \frac{\rho}{a} \exp(-\rho^2/2a^2), \tag{51}$$

and a linearly polarized Gaussian beam,

$$\mathbf{E}^{(i)}(\rho, \phi, 0) = E_0 \hat{\mathbf{x}} \exp(-\rho^2/2a^2). \tag{52}$$

For our calculations we use $\Delta = a/f = 0.5$. Figure 8 shows the results for the radially-polarized beam, where it is seen that the orthogonal basis clearly outperforms its nonorthogonal counterpart. However, the nonorthogonal basis shows an overall decrease in the error, and is still able to give fairly accurate results. Figure 9 shows the same results for the incident linearly polarized beam. For this case, the orthogonal case is still better than the nonorthogonal one, but the difference is significantly less marked. Note that the results are comparable to the ones obtained in [18].

3.6. TE-TM alternative

It was shown in the previous section that the quasi-linear polarization for the basis makes the non-orthogonal basis in particular converge slower when fitting a field with a polarization singularity in the main direction of propagation. This issue can be solved by choosing different polarization vectors. Taking $\mathbf{V}_\mathbf{u} = -\mathbf{u} \times \hat{\mathbf{z}} \times \mathbf{u}$, the polarization vectors $\mathbf{V}_\mathbf{u}$ and $\mathbf{u} \times \mathbf{V}_\mathbf{u}$ point in the polar and azimuthal directions, respectively [see Fig. 4(b)]. Following the same procedure as before but noticing that in this case $\|\mathbf{V}_\mathbf{u}\|^2 = \sin^2\theta$, we obtain an orthogonal basis where the polynomial $G_{n,m}$ now satisfies the following orthogonality condition:

$$\int_{\exp(-2q)}^{\exp(2q)} G_{n',m}(v) G_{n,m}(v) \left(1 - \frac{1}{4q^2} \ln^2 v\right)^{|m|+1} \mathrm{d}v = h_{n,m}(q) \delta_{n,n'}. \tag{53}$$

Optics EXPRESS

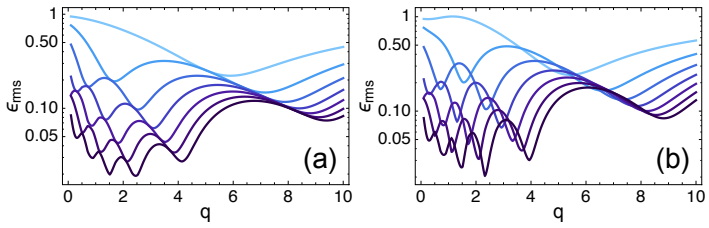

Fig. 10. Rms error as a function of q for a focused radially-polarized Laguerre-Gauss beam of order one with $\Delta = 0.5$ for the TE-TM (a) orthogonal, and (b) nonorthogonal bases with truncation orders ranging from $l_{\max} = 0$ (lighter curves) to $l_{\max} = 6$ (darker curves) and $m = 0$.

Similarly, this basis can be taken to the configuration space by means of the position representation of the polarization operator which is now given by $\mathbf{V}_\mathbf{r} = \nabla \times (\hat{\mathbf{z}} \times \nabla)$.

Additionally, we can also derive a suitable nonorthogonal basis by writing it in terms of $\cos\Theta(\theta; q)$ and taking the limit $q \to 0$. We find, again, that the $Q_{n,m}$ polynomials can be expressed in terms of the Jacobi polynomials, but in this case $P_n^{(|m|+1,|m|+1)}$ (which can be written in terms of the generalized Legendre functions if preferred). The coefficients $p_{n,m}$ would need to be modified to account for the use of different polynomials so that the basis would be orthonormal with respect to the weight

$$W_m(\theta) = \frac{[1 - \cos\Theta(\theta; q)]^{|m|+1}[1 + \cos\Theta(\theta; q)]^{|m|+1}}{(1 - \cos\theta)^{|m|+1}(1 + \cos\theta)^{|m|+1}}, \tag{54}$$

which follows a similar trend as the previous one (see Fig. 6).

Figure 10 shows the results of fitting the radially-polarized field defined in the previous section. For the nonorthogonal case we notice a clear improvement, whereas for the orthogonal basis the results are comparable to those obtained using the quasi-linear basis.

4. Final remarks

Complete bases for the description of focused scalar and electromagnetic (with several polarization distributions) fields were proposed, which constitute closed-form solutions of the wave equation in question. For each case, two options were considered: bases that are orthogonal over the directional space with uniform weight but requiring a set of non-standard orthogonal polynomials, and bases that require a directional weight factor for orthogonality but with the advantage of being expressible in terms of standard (Jacobi) polynomials. In all cases, the basis elements are linear combinations of simple vortex complex-focus fields. For this reason, we expect that they will be useful in modeling the Mie scattering off spherical particles, extending the formalism for incident CF field in [30] and for a different basis for scalar fields in [31].

A. Method of moments

Given an orthogonality relation for some $p_n(x)$ polynomials of the form

$$\int_a^b p_n(x) p_{n'}(x) w(x)\, \mathrm{d}x = h_n \delta_{n,n'}, \tag{55}$$

where $w(x)$ is a weight function, we can construct the set of orthogonal polynomials by the method of moments [23, 24]. To do this, we first need to compute the moments of the weight

Optics EXPRESS

function which are defined as

$$\mu_j = \int_a^b w(x) x^j \, \mathrm{d}x. \tag{56}$$

Note that, for all the bases treated in this work, an analytic form in terms of q can be obtained. Given these we can calculate the polynomials by means of the following determinant:

$$p_n(x) = \begin{vmatrix} \mu_0 & \mu_1 & \cdots & \mu_n \\ \mu_1 & \mu_2 & \cdots & \mu_{n+1} \\ \vdots & \vdots & \ddots & \vdots \\ \mu_{n-1} & \mu_n & \cdots & \mu_{2n-1} \\ 1 & x & \cdots & x^n \end{vmatrix}. \tag{57}$$

We can also compute their norm which is given by the inner product $h_n = \langle p_n | \, p_n \rangle = \Delta_{n-1}\Delta_n$ and their recurrence relation,

$$p_{n+1}(x) = (A_n + B_n x) p_n(x) - C_n p_{n-1}(x) \tag{58}$$

where

$$A_n = \frac{\Delta_n}{\Delta_{n-1}} \left(\frac{K_{n+1}}{\Delta_n} - \frac{K_n}{\Delta_{n-1}} \right), \quad B_n = \frac{\Delta_n}{\Delta_{n-1}}, \quad C_n = B_n^2, \tag{59}$$

with

$$\Delta_n = \begin{vmatrix} \mu_0 & \mu_1 & \cdots & \mu_n \\ \mu_1 & \mu_2 & \cdots & \mu_{n+1} \\ \vdots & \vdots & \ddots & \vdots \\ \mu_n & \mu_{n+1} & \cdots & \mu_{2n} \end{vmatrix}, \qquad K_n = \begin{vmatrix} \mu_0 & \mu_1 & \cdots & \mu_{n-2} & \mu_n \\ \mu_1 & \mu_2 & \cdots & \mu_{n-1} & \mu_{n+1} \\ \vdots & \vdots & \ddots & \vdots & \vdots \\ \mu_{n-1} & \mu_n & \cdots & \mu_{2n-3} & \mu_{2n-1} \end{vmatrix}. \tag{60}$$

Funding

National Science Foundation (NSF) (PHY-1507278).

Acknowledgments

R. Gutiérrez-Cuevas acknowledges the support of a CONACYT fellowship.

138.231.238.199 {3025-10-22 14:21}